Contrasting palaeosol development in two different tectonic settings: the Upper Buntsandstein of the Western Iberian Ranges, Central Spain

Ana. M. Alonso-Zarza , Alfonso Sopeña and Yolanda Sánchez-Moya

Palaeosols may offer excellent evidence for the development of sedimentary basins but few studies have used diagenetically altered material: here we show that material of this sort can also reflect the sedimentary environment. The Lower to Middle Triassic red beds of the western Iberian Ranges were deposited in a tectonically active half-graben in which subsidence rates varied along the basin as a response to differential fault movements. During this period the basin was filled by a set of fluvial units with interbedded palaeosols. The palaeosols show typical pedogenic calcrete profiles, although extensive dolomitization has deleted part of their microstructure; however, macrostructure and morphology are preserved. Differences in the maturity stages of the palaeosols are related to the changes in subsidence and sedimentation rates along the basin. Thus, two different scenarios are recognized at: (i) the hanging wall, Riba de Santiuste area, where palaeosols reach stage III as the episodic tilting of the floodplain inhibited the development of more mature soils and (ii) the footwall, Cercadillo area, where palaeosols attain stage V maturity, favoured by prolonged periods of tectonic stability resulting in lower sedimentation rates over the floodplain areas.

Introduction

In the last 15 years it has been clearly shown that fluvial architecture, and the micro-/macrostructure and distribution of palaeosols are closely linked (e.g. Kraus, 1987; Alonso-Zarza *et al.*, 1992; Mack *et al.*, 1994; Wright and Marriot, 1996; Kraus, 1997). Establishing these relationships has allowed a better understanding of continental basins focusing on their tectonic, climatic, and in some cases, sea-level histories. However, most of the cases studied analyse palaeosols that do not show important diagenetic modifications, such as the Eocene Willwood Formation (e.g. Bown and Kraus, 1981) or the Miocene palaeosols of the Madrid Basin (Alonso-Zarza *et al.*, 1992).

The Lower to Middle Triassic deposits of the Iberian Ranges (Fig. 1) contain a set of palaeosols that have been extensively dolomitized and so many of the primary pedogenic features are not preserved. However, a variety of large- and small-scale features can still be recognized after dolomitization, which can indicate differences in fluvial and tectonic settings. In this context two distinctive scenarios are studied in relation to fault system evolution and, therefore, subsidence rates: fluvial architecture, and palaeosol development.

Geological setting and alluvial architecture

This paper focuses on the upper Bundtsandstein (Lower-Middle Triassic) of the western Iberian trough border (Riba de Santiuste anticline, Central Spain), where deposition, within a fault-bounded half-graben, took place in a widespread axial type fluvial system and local alluvial fans. The multibend nature of the master fault and the differences in synsedimentary slip on the different fault segments exerted a decisive control on subsidence distribution and fluvial architecture evolution. The geometry of the basin and fluvial sedimentology have been established through the detailed mapping of the terrestrial units (Sánchez-Moya *et al.*, 1996) (Fig. 1). Figure 2 shows a correlation chart and the stratigraphic architecture of the Triassic in the studied area. Within the Buntsandstein units, the best-developed palaeosols occur in unit F-3 (Fig. 1) deposited within a sandy fluvial system. During the sedimentation of this unit the fault-induced subsidence rate in the hanging wall, controlled by rollover growth, was higher than in the footwall. The change in general stratal geometry from retrogradational to nearly parallel suggests the evolution from mainly rollover growth to dominant displacement on the major faults of the basin margins related to final syntectonic episodes of the rifting (Sánchez-Moya *et al.*, 1996).

The deposits of this unit show a simple external geometry but a very complex internal stratal pattern with small discontinuities, erosional unconformities, and palaeosol profiles. The fluvial deposits have a variety of deeply entrenched channels (6–10 m deep) that are large tabular-lenticular bodies, separated by minor fine-grained units. The overbank deposits consist mainly of massive red mudstones with common palaeosol horizons developed across the floodplain. Crevasse channel, crevasse splay, and levees are also common. These characteristics suggest the predominance of sandy braided alluvial conditions with a low braiding index. Two distinctive scenarios related to fault system evolution and subsidence rate controlled the fluvial architecture and palaeosol development (Fig. 2). The eastern example, the Riba de Santiuste area corresponds to the hanging wall block (Fig. 2) and shows an evolution of different fluvial sequences in relation to instantaneous tilt triggered by individual extensional tectonic events. In this area the fluvial

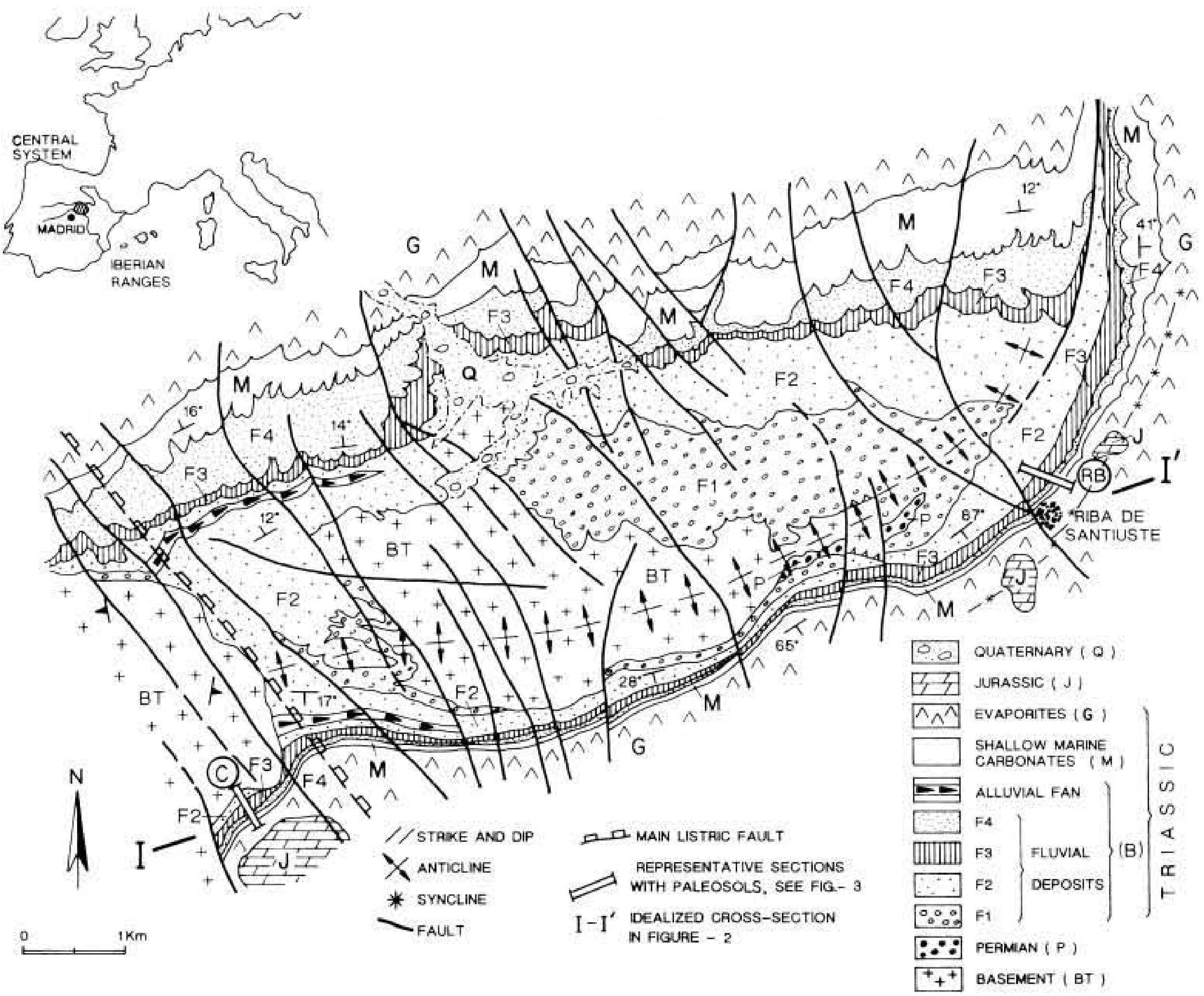

Fig. 1 Geological setting of the study area. The map shows the different formations recognized and the location of the Riba de Santiuste (RB) and Cercadillo (C) sections.

deposits reflect the predominance of a sandy braided system, characterized by a relatively mobile channel belt. Within each fluvial sequence the channel belt moved over the floodplain from NE to SW. The total thickness of the fluvial sequence is 223 m and it has up to eight palaeosols. The Cercadillo area was by that time on the footwall block (Fig. 2), with lower subsidence rates, indicated by the reduced thickness (60 m) of the fluvial sequence and only one palaeosol. The fluvial sediments indicate a more stable, but shallower, channel belt and a predominance of interchannel-floodplain areas. There is no evidence of channel incision or terraces, probably because sedimentation kept pace with subsidence or slightly outpaced it.

Triassic palaeosols

In all the palaeosols studied the primary mesoscale structure is well preserved; however, study of thin sections, mineralogy, SEM, and geochemistry confirms that the initial composition is not preserved due to replacement of the soil calcite by dolomite. The carbonate of the palaeosols is ferroan dolomite. Microprobe analyses have shown that the $CaCO_3$ content in the dolomite lattice is 50.9 mol %, $MgCO_3$: 45.2 and $FeCO_3$: 4.4 (mean values).

In the Riba de Santiuste area, the hanging-wall, palaeosols reach up to stage III of Machette's (1985) classification. The basal contact is gradational with the red clays that constitute the host rock (Fig. 3). The top of the profile is sharp and is overlain by red clays or sharply cut by fluvial channel or crevasse-splay deposits. Maximum thickness of the individual profiles is 2 m. The transition from the host to the palaeosol is always gradual as well as the boundaries between the different horizons, while tops of the profiles are very sharp. Palaeosols can be traced laterally up to several hundred metres.

The soil profiles in the Riba de Santiuste area (Fig. 4) consist on a lower horizon of red clays with scattered dolomite nodules (Fig. 3). Nodules are cylindrical to spherical and about 3 cm in diameter. Green mottling is very prominent and relict bedding is commonly preserved at the base of the horizon. The upper horizon is typically nodular and up to 0.8 m thick. It con-

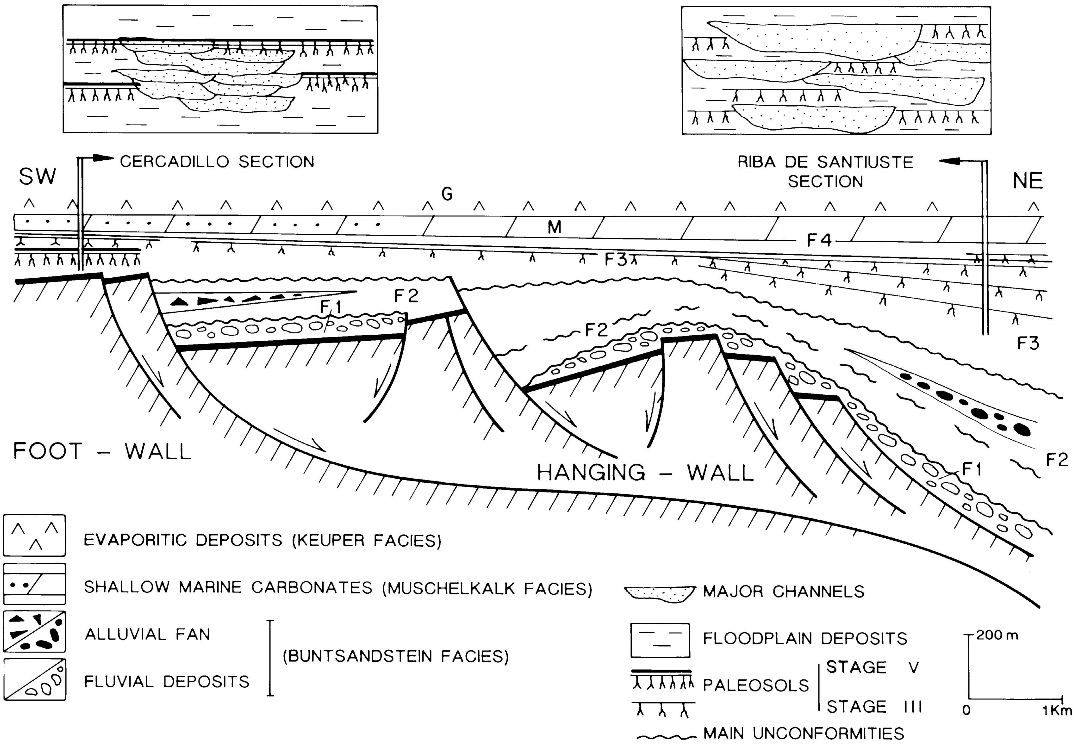

Fig. 2 Sketch showing the geometry of the basin and the different tectonic setting of the two studied areas, Cerdadillo (left) and Riba de Santiuste (right). Comparison of fluvial architecture and palaeosol development on hanging wall and footwall blocks.

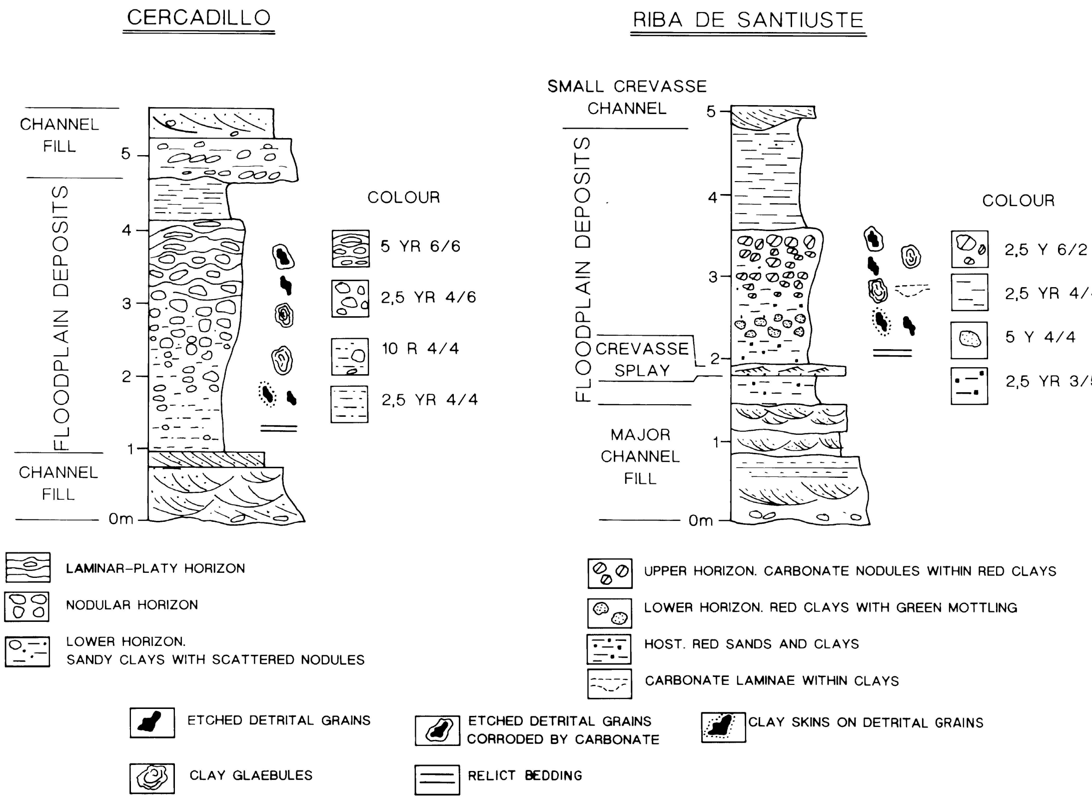

Fig. 3 Partial measured logs of Cercadillo and Riba de Santiuste. The palaeosols contained in each section are representative of the palaeosol recognized in each area.

sists of spherical and prismatic dolomite nodules up to 10 cm in diameter separated from each other by films of red-green clays.

In the Cercadillo area, the footwall, the only profile is thicker (3 m) and consists of three different horizons (Fig. 3 and 5). We have studied in detail a palaeosol developed in, and overlain by, red clays. This palaeosol can be traced laterally for several kilometres. The base is gradational and the top is sharp. Transitions between the three horizons are also gradational. The two lower horizons are very similar to those described previously, except that green mottling is absent or less prominent. The uppermost horizon is about 1 m thick and is formed of irregular and wavy laminae up to 15 cm in thickness (Fig. 5). The morphological stage of the profile is V (Machette, 1985), as it has a laminar cap thicker than 1 cm. Here the red clays form irregular laminae within the dense dolomite mosaics. Some fine laminations of carbonate are preserved within the clays and resemble small-scale laminae commonly recognized in incipient laminar calcretes.

Microfabrics typically recognized in calcretes are common in these profiles, but not always easy to identify due to the replacement by dolomite, which erased some of the primary microstructure. Lower horizons show scarce pedogenic modification and lamination and orientation of the detrital grains is preserved. Etched detrital grains and clay cutans are the dominant pedogenic microfeatures. Some thin and irregular carbonate laminae disrupt the original fabric (Fig. 6). These laminae are similar to those described in incipient laminar calcretes in Neogene detrital deposits, which have been interpreted as calcified root structures (Alonso-Zarza, 1999). The nodular horizon comprises a dense mosaic of dolomite with a mean crystal size of 0.2 mm. Dolomite nodules are separated from each other by clays (Fig. 7). Clay glaebules up to 1 mm in diameter occur irregularly in the dolomite mosaics. Glaebules consist of illite and etched quartz grains. Some clays are orientated showing a skelsepic fabric. Relicts of iron oxides, clay glaebules, and detrital quartz grains are common all along these nodular horizons. Micritic filaments rarely coated by Fe-oxides are seen connecting some of the dolomite nodules. In the platy upper horizons, clays form irregular laminae within the dense dolomite mosaics. Clays show strong orientation and fabrics ranging from mosepic to masepic (Brewer, 1964). Dolomite crystals tend to be more euhedral and larger, about 0.4 mm across. In all the horizons of the profile, the dolomite crystals show inclusions of anhydrite. Cements of gypsum, dolomite, and calcite are common.

Interpretation and discussion

Morphology of the soil horizons and their relationships with the host rock, gradational bases and sharp tops, all indicate clearly that these palaeosols are mostly pedogenic in origin. Calcite was probably the primary precipitate within the soil, but was later replaced by dolomite. The dolomitization erased most of the primary microfabrics with the exception of the relict clay glaebules, detrital etched grains, and fine laminae within the clays. Another argument in favour of pedogenic origin is the fact that these dolocretes in the Riba de Santiuste area pinch out in the proximity of the channels and thicken with distance from them, indicating a pedofacies relationship (Bown and Kraus, 1987), which has not been recognized in the Cercadillo area.

Palaeosol geometry, arrangement, and characteristics have been used in basin analysis as indicators of sedimentation and/or subsidence rates (Atkinson, 1986; Wright and Marriot, 1996), basin morphology (Mack and James,

Fig. 4 (Left) Riba de Santiuste profile showing two horizons: 1, Lower horizon of sandy clays with scattered dolomite nodules. 2, Upper horizon with coalescent nodules. Visible scale bar is 60 cm.

Fig. 5 (Above) Cercadillo profile showing three different horizons: 1, Lower horizon composed of sandy clays with scattered dolomite nodules. 2, Nodular horizon with the nodules arranged vertically. 3, Platy horizon. Scale bar is 2 m.

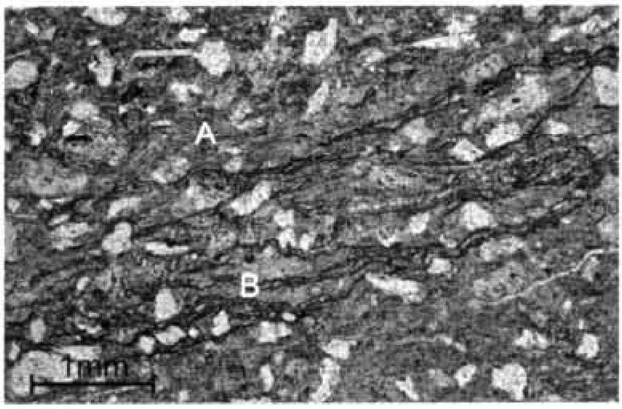

Fig. 6 Photomicrograph of the lower horizon formed by sandy clays and etched detrital grains (A). The irregular carbonate laminae (B) cut and corrode the siliciclastic host rock.

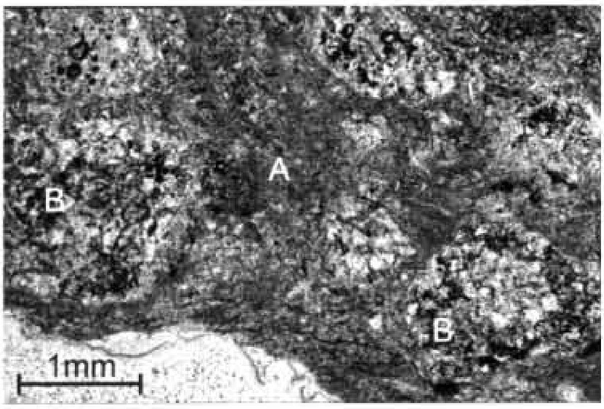

Fig. 7 Nodular horizon. The red clays (A) that constitute the host rock are displaced around the carbonate nodules (B).

1993), fluvial architecture (Kraus and Gwinn, 1997), palaeoclimate (Goodfriend and Magaritz, 1988; Retallack and Alonso-Zarza, 1998) and vegetation (Retallack, 1997). In this study we show two different areas of the same basin in which palaeosol maturity and lateral extent show significant changes related to the interplay of the different soil formation factors (Jenny, 1941).

Time

The evaluation of the time that the palaeosols represent within a fluvial sequence is difficult and somewhat controversial. Detailed chronological studies required to obtain precise data are hard to obtain in Triassic continental facies. Palynological associations obtained in previous studies (Sopeña *et al.*, 1995) indicate a general age of Anisian lower Ladinian for these deposits. It has not been possible to obtain more precise chronological data, so in order to have an idea of the time represented by the palaeosols we use the morphological stage of development of the soils, because in noncalcareous parent sediments it is related directly to the length of time in which the palaeosol developed (Gile *et al.*, 1966, 1981). Calcic palaeosols of stage II may form over thousands of years, stage III soils require from tens of thousands to hundreds of thousands years, stage IV soils require several hundred thousand to a half million years, and longer periods yet are needed for stages V and VI (Gile *et al.*, 1981). These figures are similar to those used in other alluvial sequences, such as the Tertiary of the Loranca Basin in Spain (Daams *et al.*, 1996) or the Tertiary of South Dakota (Retallack, 1984). However, when comparing absolute chronological data obtained through palaeomagnetic or radiometric studies, with those obtained from the study of the time of formation of palaeosols and sedimentation rates of the associated deposits, important differences are observed; even so, the obtained results may be good in relative timing (Retallack, 1984). The differences between the two types of data may be due to the highly variability in fluvial sedimentation (Daams *et al.*, 1996) or to the different time that palaeosols with the same maturity stages may represent when formed under different climate, vegetation or source rock. For example, it has been suggested that the formation of biogenic or 'β-calcretes' is faster than the formation of calcretes in which biogenesis played a minor role or is absent (Wright, 1990). In short, it is difficult to assess a time of formation for the palaeosols of the two sections studied. However, as the climate, source rock, and vegetation should have been similar throughout the study area, the only two soil formation factors which may have varied from one area to the other are relief and time. These two factors are closely related, as variations in relief account for changes in sedimentation rates and also for different time for soil formation processes, as discussed below.

Tectonism

Differences in soil development and micromorphology can be explained by differences in the subsidence rates controlling the architecture and the sedimentation rate within the fluvial systems. In the Riba de Santiuste area, episodic tilting (Sopeña and Sánchez-Moya, 1997) of the floodplain resulted in periods of sedimentation followed by short periods of stabilization, which were favourable conditions for the development of not very mature palaeosol profiles. The occurrence of extensive mottling indicates relatively high groundwater due to the rapidly aggrading floodplain caused by high subsidence rates. In this area pedogenic processes probably interacted with phreatic ones. Tectonic instability, reflected in the episodic titling of the hanging wall may be considered as the main factor that accounted for the formation of less mature palaeosols in this area of the basin.

On the other hand, in the footwall (Cercadillo) area, prolonged periods of tectonic stability resulted in lower sedimentation rates that allowed the development of more mature palaeosols. In the profile from Cercadillo, the occurrence of a laminar horizon at the top and the fact that this dolocrete is laterally very extensive suggest a relatively mature dolocrete that can be compared with laminar calcretes developed in relatively stable and flat surfaces (e.g. Sancho and Meléndez, 1992; Alonso-Zarza *et al.*, 1998a) and so its presence reflects an important sedimentary discontinuity or a condensed footwall section. Condensed fluvial sequences with mature palaeosols have been recognized in a similar situation in the southern Rio Grande rift, where cessation of fluvial sedimentation in the footwall block of the Doña Ana Mountains accounted for the development of mature soils, whereas in the hanging wall continued sedimentation allowed the development of immature palaeosols (Mack *et al.*, 1994).

Climate and vegetation

Calcretes have been commonly considered as indicators of arid or semiarid climates where rainfall is between 400 and 600 mm, but in the case of limestone parent rocks calcrete may form with annual rainfall in excess of 1500 mm (Goudie, 1983). There is no evidence in this study of calcareous parent sediment. In more arid climates gypcretes tend to form, even if source rocks are not gypsiferous; the absence of pedogenic gypsum indicates a semiarid climate. Evidence for seasonality, such as pseudoanticlines and slickensides characteristic of Vertisols (Allen, 1986) are not recognized in this area, but this may also be due to the lack of expandable clays.

Evidence for Triassic vegetation is based on palynological studies, which have shown the dominance of gymnosperms (mostly conifers) and Equisetum (Sopeña *et al.*, 1995). More information on vegetation can be obtained through the microstructure of the calcretes. In our case some ghosts of organic structures, such as micritic filaments, probably of fungal origin, as well as some spherical bodies attributed to bacteria, are the only biogenic remains that are preserved, after extensive dolomitization. These features, together with the laminar structures of the Cercadillo profile, suggest that the vegetation played an important role in the formation of the primary calcrete as shown in more recent laminar calcretes (e.g. Monger *et al.*, 1991; Alonso-Zarza *et al.*, 1998a, b).

Diagenesis

We have not carried out any specific work on the diagenesis of these calcretes as the precise geochemical data needed to interpret correctly the diagenetic pathways and their geochemical characteristics is beyond the remit of this contribution. Our petrographic study shows that, in most cases, the sequence of diagenetic processes is: dolomitization, precipitation of gypsum/anhydrite cement and late spar calcite, which may indicate that the dolomitization was probably driven by mixing of meteoric and marine waters. Dolomitization caused a decrease in the Mg/Ca ratio of the pore water enabling the precipitation of sulphate minerals. Mixing-water dolomitization models have been commonly proposed to explain either the dolomite cementation of Triassic sandstones of the Iberian Ranges (Morad *et al.*, 1992) or the dolostones of the Muschelkalk carbonate ramp in the SE Iberian Ranges (López-Gómez *et al.*, 1993). Late influence of meteoric waters caused the precipitation of the coarse calcite spar cements.

Conclusions

The palaeosols from the Triassic of the Iberian Ranges show typical pedogenic profiles, even if the primary fabric is not well preserved. This is important because, even with the loss of primary features by dolomitization, palaeosol features in relation to the fluvial system support different subsidence rates and tectonic settings for the two studied areas. However, extensive dolomitization does not allow any significant inference on climate or vegetation in this area during the lower Triassic.

Acknowledgements

This work has been supported by Dirección General de Enseñanza Superior e Investigación Cientifica through the Project PB-97–1208. Dr G.J. Retallack and his laboratory of the University of Oregon are thanked for the help in thin section preparation. Drs Gierlowski-Kordesch, Mack and Wright are thanked for the careful and constructive reviews of the manuscript.

References

Allen, J.R.L., 1986. Pedogenic calcretes in the Old Red Sandstone Facies (Late Silurian-Early Carboniferous) of the Anglo-Welsh area, Southern Britain. In: *Paleosols. Their Recognition and Interpretation* (V.P. Wright, ed.), pp. 58–86. Blackwell Scientific Publications, Oxford.

Alonso-Zarza, A.M., 1999. Initial stages of laminar calcrete formation by roots. *Sediment. Geol.*, **126**, 177–191.

Alonso-Zarza, A.M., Silva, P.G., Goy, J.L. and Zazo, C., 1998a. Fan-surface dynamics and biogenic calcrete development: Interactions during ultimate phases of fan evolution in the semiarid SE Spain (Murcia). *Geomorphology*, **24**, 147–167.

Alonso-Zarza, A.M., Sanz, M.E., Calvo, J.P. and Estévez, P., 1998b. Calcified root cells in Miocene pedogenic carbonates of the Madrid Basin: evidence for the origin of *Microdocodium* b. *Sediment. Geol.*, **116**, 81–97.

Alonso-Zarza, A.M., Wright, V.P., Calvo, J.P. and García del Cura, M.A., 1992. Soil-landscape relationships in the Middle Miocene of the Madrid Basin. *Sedimentology*, **39**, 17–35.

Atkinson, C.D., 1986. Tectonic control on alluvial sedimentation as revealed by an ancient catena in the Capella Formation (Eocene) of Northern Spain. In: *Paleosols. Their Recognition and Interpretation* (V.P. Wright, ed.), pp. 139–179. Blackwell Scientific Publications, Oxford.

Bown, T.M. and Kraus, M.J., 1981. Lower Eocene alluvial paleosols (Willwood Formation (Lower Eocene), Bighorn Basin, northwest Wyoming, U.S.A. *Palaeogeogr. Palaeoclim. Palaeoecol.*, **43**, 95–128.

Bown, T.M. and Kraus, M.J., 1987. Integration of channel and floodplain suites in aggrading fluvial systems, I. Developmental sequence and lateral relations of lower Eocene alluvial paleosols, Willwood Formation, Bighorn Basin, Wyoming. *J. Sediment. Petrol.*, **57**, 587–601.

Brewer, R., 1964. *Fabric and Mineral Analysis of Soils*. Wiley, London.

Daams, R., Díaz-Molina, M. and Más, R., 1996. Uncertainties in the stratigraphic analysis of fluvial deposits from the Loranca Basin, central Spain. *Sediment. Geol.*, **102**, 187–209.

Gile, L.H., Hawley, J.W. and Grossman, R.B., 1981. Soils and geomorphology in the Basin and Range area of southern New Mexico-Guidebook of the Desert Project. *New Mexico Bur. Mines Min. Res. Mem.*, **39**, 222p.

Gile, L.H., Petterson, F.F. and Grossman, R.B., 1966. Morphological and genetic sequences of carbonate accumulation in desert soils. *Soil Sci.*, **101**, 347–360.

Goodfriend, G.A. and Magaritz, M., 1988. Paleosols and late Pleistocene rainfall fluctuations in the Negev Desert. *Nature*, **332**, 144–146.

Goudie, A.S., 1983. Calcrete. In: *Chemical Sediments and Geomorphology* (A.S. Goudie and K. Pye, eds), pp. 93–131. Academic Press, London.

Jenny, K., 1941. *Factors in Soil Formations*. McGraw-Hill, New York, 281 pp.

Kraus, M.J., 1987. Integration of channel and floodplain suites in aggrading alluvial systems, II. Vertical relations of lower Eocene paleosols, Willwood Formation, Bighorn Basin, Wyoming. *J. Sediment. Petrol.*, **57**, 602–612.

Kraus, M.J., 1997. Lower Eocene alluvial paleosols: Pedogenic development, stratigraphic relationships, and paleosol/ landscape associations. *Palaeogeogr. Palaeoclim. Palaeoecol.*, **129,** 387–406.

Kraus, M.J. and Gwinn, B., 1997. Facies architecture of Paleogene floodplain deposits, Willwood Formation, Bighorn Basin, Wyoming, USA. *Sediment. Geol.*, **114,** 33–54.

López-Gómez, J., Más, R. and Arche, A., 1993. The evolution of the Middle Triassic (Muschelkalk) carbonate ramp in the SE Iberian Ranges, eastern Spain: sequence stratigraphy, dolomitization processes and dynamic controls. *Sediment. Geol.*, **87,** 165–193.

Machette, M.N., 1985. Calcic soils of southwestern United States. In: *Soil and Quaternary Geology of the Southwestern United States* (C.L. Weide, ed.). *Spec. Pap. Geol. Soc. Am.*, **203,** 1–21.

Mack, G.H. and James, W.C., 1993. Control on basin symmetry on fluvial lithofacies, Camp Rice and Palomas Formation (Plio-Pleistocene), sourthern Rio Grande rift, USA. *Spec. Publs Int. Ass. Sediment.*, **17,** 439–449.

Mack, G.H., James, W.C. and Salyards, S.L., 1994. Late Pliocene and early Pleistocene sedimentation as influenced by intrabasinal faulting, southern Rio Grande rift. In: *Basins of the Rio Grande Rift: Structure, Stratigraphy, and Tectonic Setting* (G.R. Keller and S.M. Cather, eds). *Spec. Pap. Geol. Soc. Am.*, **291,** 257–263.

Monger, H.C., Dougherty, L.A., Lindemen, W.C. and Lidell, C.M., 1991. Microbial precipitation of pedogenic carbonate. *Geology*, **19,** 997–1000.

Morad, S., Marfil, R., Al-Aasm, I.S. and Gómez-Grass, D., 1992. The role of mixing-zone dolomitization in sandstone cementation: evidence from the Triassic Buntsandstein, The Iberian Range, Spain. *Sediment. Geol.*, **80,** 53–65.

Retallack, G.J., 1984. Completeness of the rock and fossil record: some estimates using fossil soils. *Paleobiology*, **10,** 59–78.

Retallack, G.J., 1997. Neogene expansion of the North American Prairie. *Palaios*, **12,** 380–390.

Retallack, G.J. and Alonso-Zarza, A.M., 1998. Middle Triassic paleosols and paleoclimate of Antarctica. *J. Sediment. Research*, **68,** 169–184.

Sánchez-Moya, Y., Sopeña, A. and Ramos, A., 1996. Infill architecture of a nonmarine half-graben Triassic Basin (Central Spain). *J. Sediment. Research*, **66,** 1122–1136.

Sancho, C. and Meléndez, A., 1992. Génesis y significado ambiental de los caliches Pleistocenos de la región del Cinca (Depresión del Ebro). *Rev. Soc. Geol. España*, **5,** 81–93.

Sopeña, A., Doubinger, J., Ramos, A. and Pérez-Arlucea, M., 1995. Palynologie du Permien et du Trias dans le Centre de la Péninsule Ibérique. *Sci. Géol. Bull.*, **48** (1–3), 119–157.

Sopeña, A. and Sánchez-Moya, Y., 1997. Tectonic systems tract and depositional architecture of western border of the Triassic Trough (central Spain). *Sediment. Geol.*, **113,** 245–267.

Wright, V.P., 1990. Estimating rates of calcrete formation and sediment accretion in ancient alluvial deposits. *Geol Mag.*, **127,** 273–276.

Wright, V.P. and Marriot, S.B., 1996. A quantitative approach to soil occurrence in alluvial deposits and its application to the Old Red Sandstone of Britain. *J. Geol Soc. London*, **153,** 907–913.